OPTIMIZATION OF CONDUCTIVE AND ELECTROACTIVE POLYMER HYDROGELS AS ELECTROACTIVE MUSCLE SCAFFOLDS

By

ZALIKATU KAMARA

A thesis submitted to the

School of Graduate Studies

Rutgers, The State University of New Jersey

In partial fulfillment of the requirements

For the degree of

Master of Science

Graduate Program in Biomedical Engineering

Written under the direction of

Joseph W. Freeman

And approved by

_____

_____

_____

_____

New Brunswick, New Jersey

January 2023

ABSTRACT OF THE THESIS

OPTIMIZATION OF CONDUCTIVE AND ELECTROACTIVE POLYMER HYDROGELS AS ELECTROACTIVE MUSCLE SCAFFOLDS

By ZALIKATU KAMARA

Thesis Advisor:

Joseph W. Freeman

Skeletal muscles have great regeneration abilities after small wounds or injuries. However, in extreme cases with chronic damage, and traumatic injuries, the regenerative properties of skeletal muscle can be hindered. Biocompatible material muscle grafts such as electroactive muscle scaffolds are currently studied as an alternative treatment method. Electroactive muscle scaffolds serve as great alternatives because of their ability to mimic native muscle with its mechanical and contractile properties. We can produce active materials that contract and expand as needed, much like skeletal muscle, by strategically placing conductive elements around electroactive polymer (EAP) hydrogels. These ideas can be combined to produce active materials that can electrically, physically, and biochemically activate cells. Their design allows them to function similarly to native muscle when electrically stimulated by converting polymer bending into overall scaffold contraction. The electroactive and conductive portions of the muscle scaffold are needed to stimulate the actuation and contraction of the scaffold. The electroactive portion is

made with an electroactive polymer made from polyethylene glycol diacrylate (PEGDA) and acrylic acid (AA). The conductive portion can be created with several different conductive materials combined with PEGDA. In this study, we investigated the use of carbon nanotubes, gold nanoparticles, and $FeCl_3$ as conductive elements for our scaffolds. These elements were combined with PEGDA alone and PEGDA-AA. Results show a concentration-based change in mechanical properties and conductivity with the addition of these elements. These materials were able to create electric fields strong enough to move the electroactive material PEGDA-AA.

Dedication

To my parents, my rock

Acknowledgments

First and foremost, I would not be where I am today without God's guidance and protection. I thank him for how far he has bought in my academic journey. To Dr.Freeman, thank you for accepting me into your lab, as an undergraduate. I have learned so much and grown since then. I have been able to work on two projects, and work with many people, and learn an endless amount of knowledge. Thank you for always pushing me and offering words of encouragement during my struggles in the lab, and graduate school. I am forever grateful for all the help and encouragement you have given me over the years. Thank you to my fellow MoTR lab mates. Shreya Madhavarapu for taking me in as undergraduate and helping through the ropes of the bone project. Mike Pellegrini for helping me out with just about anything, especially with all my cell work. Brandon Newton for bringing me on to the muscle project and teaching me the basics. I would also like to thank all the undergraduate students that have offered help, and advice especially through the most frustrating times with the 3D printer. Additionally I would like to thank Dr.Labazzo, and Dr.Mao for serving on my thesis committee. And last but certainly not least I would like to thank my family and friends for getting me through this. I would not be here without you all. Thank you to my brother and sister for the endless support. And to my mom and dad for reminding everyday that I could do this, God was behind me, and supporting me in every step I made regardless of the setbacks I had. Thank you, thank you, thank you!

TABLE OF CONTENTS

LIST OF FIGURES

CHAPTER 1 - Introduction

1.1 Skeletal Muscle Regeneration

The process of the regeneration of skeletal muscle is a difficult task to complete after the loss of muscle following chronic damage or traumatic injuries. Skeletal muscles have great regeneration abilities when it comes to small wounds or injuries. However, in extreme cases with chronic damage, and traumatic injuries where there are large volume defects, the regenerative properties of skeletal muscle can be difficult to accomplish. Skeletal muscle has the capacity to replace damaged tissue after injury up to a certain point. The residual muscle tissue cannot entirely recover its function after passing this capacity.[21] This is because of the complicated nature and unique mechanical and electrical properties of skeletal muscle.

1.2 Skeletal Muscle Function and Structure

The four primary purposes of skeletal muscles are to produce movement, maintain posture and placement, regulate body temperature, store nutrients, and stabilize joints.[1] The structural design of skeletal muscle enables effective force production. Sarcomeres, which contain myosin and actin and form overlaps to enable muscle contraction, are the most fundamental structural units of a myofiber (9). In striated muscle, the Z-band (Z-line, Z-disc) divides the I-band of adjacent sarcomeres and marks the sarcomere's boundary. There are two locations in the sarcomere where myofilaments are crosslinked to preserve interfilament spacing and axial register, one being the Z-band, and the other the M-band at the center of the A-band, where myosin filaments are crosslinked (4). Adenosine triphosphate (ATP) hydrolysis from actin binding to myosin allows myosin to be pulled along, shortening the sarcomere and causing muscular contraction.[18]

1.3 Large Muscle Volume Defects

However, muscle damage is not limited to trauma and injury, but can also be a result of inherited genetic illnesses or metabolic problems. A set of disorders known as muscular dystrophies result in gradual muscle loss and weakening. One of which is Duchenne muscular dystrophy.[6] Sarcopenia is a degenerative disease linked to metabolic conditions like metabolic syndrome which also leads to muscle loss.[7] In extreme cases of muscle loss injuries, limb amputations are required. Limb loss is a growing issue because almost 2 million people are living with it in the United States alone.[24] And roughly around 185,000 amputations yearly in the United States.[14] Reducing the number of amputations by limiting muscle volume defects after injuries can prevent extensive muscle damage and limb loss.

1.4 Components to Muscle Regeneration

Regeneration of muscle is difficult in large-volume defects because of the loss of necessary regenerative cellular components and the complicated nature and unique mechanical and electrical properties of skeletal muscle. Muscle regeneration is primarily regulated by ECM proteins and secreted factors, and depends on the number of satellite cells, interstitial cells, and blood vessels.[5] In addition to the biological need for muscle regeneration, there is also a need for electrical and mechanical stimulation. An essential modulator of tissue development is electrical stimulation. A key component of the physiological surroundings of the muscle is stimulation by nearby neurons. Electrical stimulation greatly accelerates sarcomere formation in muscle cell cultures .[8]

1.5 Current Solutions

Surgical intervention is called upon in cases of chronic damage, and traumatic injuries where there are large volume defects. To promote muscular tissue regeneration autografts and allografts are used. To restore the compromised function, the surgeons graft healthy muscle from a donor

spot untouched by the injury.[9] Autografts and allografts have their disadvantages which include issues with availability, high costs, immune response complications or rejection, donor site morbidity, and disease transmission. Autografts remain the most popular standard, but it is an expensive procedure that can lead to donor site morbidity, and there is a limit to how much tissue you can harvest. Allografts present a greater risk for immune reaction and infection and reduced regenerative properties with no cellular component. A decline in skeletal muscle mass can be prevented by exercise.[10] Physical therapy is a minimally invasive alternative to surgical procedures for promoting muscle tissue repair and regeneration. It is used frequently to treat chronic muscle loss, recover from injuries, and transfer muscle tissue. Biocompatible material muscle grafts are currently studied as alternatives to these current standards. These muscle grafts aim to mimic native muscle with its biological, mechanical, and electrical properties. The grafts' ability to provide a structural and metabolic foundation for muscle loss is promising but not as much so for large-volume defects.[11]

1.6 Proposed Solutions

Muscular tissue engineering is a rising field that aims to combat the limitations and complications of the regenerative properties of muscular tissue to large muscle volume defects with current standard treatments. Skeletal muscle tissue engineering has much promise through the use of hydrogel as a scaffold to support progenitor/stem cells for muscle differentiation and reconstruct the natural skeletal muscle tissue architecture, which is influenced by the matrix's mechanical and physical properties as well as by a dynamic environment, skeletal muscle tissue engineering holds great promise for the treatment of muscle regeneration.[15] Because of their permeable and highly hydrated structures, hydrogels are frequently employed in several biological applications as their environment is similar to the extracellular matrix of skeletal

muscle tissues. Electroactive polymers (EAP) are currently being studied for the use of artificial muscles because they have a variety of appealing qualities, including low weight, fracture tolerance, and pliability. EAP materials work similarly to biological muscles in that they are resilient, damage-tolerant, and capable of withstanding enormous actuation strains like contracting and bending.[2] Conductive polymers are also utilized in bioactive scaffolds for regenerating tissue. Because of their great conductivity, cells or tissue cultivated on them can be activated by electrical signals.[18] It has been shown that conductive biomaterials encourage the growth and differentiation of electrical stimulus-responsive cells, such as muscle cells.[11]

1.7 Aim of the Project

We propose that the combined effects of electroactive and conductive polymers will simulate muscle contraction by combining the effects of mechanical and electrical stimuli. Doing so we observe new conductive polymer composite for muscular applications, which include gold particles, carbon nanotubes, and $FeCl_3$. Carbon nanomaterials are one of the most common conductive biomaterials and have been known to be beneficial in the production of artificial muscle because of their ability to be powered by electrochemical cues.[19] Gold particles are also common conductive material because of their excellent biocompatibility, promotion of differentiation in muscle cells, and electrical conductivity.[12] Metal nanoparticles like $FeCl_3$ serve excellent electrical and conductive properties.[23] To optimize a 3D printed conductive electroactive polymer hydrogel for artificial muscle, the conductivity, resolution, biocompatibility, and actuation of CNT, gold nanoparticle, and $FeCl_3$ hydrogels were investigated.

Chapter 2- Conductive and Electroactive Polymer Hydrogel Fabrication, Conductivity, Resolution, Biocompatibility, Actuation

2.1 Materials and Methods

2.1.1 Fabrication of Electroactive Hydrogels

Electroactive Polymers were created by crosslinking polyethylene glycol diacrylate (PEGDA) with acrylic acid (AA) and a photoinitiator catalyst. The PEGDA MW 8000, was purchased from Thermo Fisher, and the photoinitiator catalyst was created with 2,2-Dimethoxy-2-phenylacetophenone and 1-Vinyl-2-pyrrolidinone were purchased from Sigma Aldrich. Hydrogels were created by dissolving PEGDA 8000 in phosphate buffered saline (PBS) at a 1:10 ratio using a vortex mixer. AA is then added to the solution at a 1:1 ratio and again mixed using a vortex mixer. A 2 ml solution is made by dissolving 0.1 grams of PEGDA 8000 into 1 ml of PBS, AND 1 ml of AA is added. The photoinitiator catalyst is formed by dissolving 0.030 grams of 2,2-Dimethoxy-2 phenylacetophenone into 100 microliters of 1-vinyl-2 pyrrolidinone. 60 microliters of the photoinitiator catalyst are added to the 2 ml PEGDA/AA solution in the dark to complete the solution. This solution is then inserted between two glass slides or poured into a PDMS old and crosslinked for two minutes. The cross-linking process occurs by exposing the glass slides or mold to UV light at a wavelength of 365 nm for two minutes.[19]

2.1.2 Fabrication of CNT Hydrogels

CNT Hydrogels are prepared similarly to PEGDA hydrogels. However, the measurements vary depending on the percent concentration of CNT that is made. The CNT solution is created at 0.05 w/v% CNT to Dimethylformamide(DMF). Hydroxylated multiwall carbon nanotubes at a diameter of >50nm were purchased from Xfnano and were added to DMF purchased from Sigma Aldrich. 0.025g of CNT is added to 50 ml of DMF. The CNT/DMF solution is then added to the PEGDA solution at varying concentrations from 1-50%.

2.1.3 Fabrication of Gold Hydrogels

Gold Hydrogels are prepared similarly to the PEGDA hydrogels. However, the measurements vary depending on the percent concentration of gold nanoparticles that are added to the solution. The 10 nm gold nanoparticles suspended in the citrate buffer were purchased from Sigma Aldrich and added to the PEGDA solution at varying concentrations from 1-50%.

2.1.4 Fabrication of $FeCl_3$ Hydrogel

$FeCl_3$ Hydrogels are prepared the same as the PEGDA hydrogels. To create the $FeCl_3$ hydrogels, the regular hydrogels are soaked in $FeCl_3$ solution overnight. The solutions were made at varying concentrations from 1-50% and $FeCl_3$ was dissolved in distilled water.

2.2 Optimization Tests

2.2.1 Conductivity of Hydrogels

The conductivity of the regular, CNT, gold nanoparticle, and $FeCl_3$ hydrogels were collected. The hydrogels were cut into 4 samples shaped as a square with a length and width of 1 cm. The hydrogels are placed on surfboard 6000 series purchased from ElectronixExpress. The hydrogel and surfboard are placed in a clamp and four electrodes are attached to them. Two electrodes from the DC power supply and 2 electrodes from the voltmeter are set at resistance. The DC power supply is set at 20 volts, and the resistance is measured. Conductivity is measured by taking the inverse of the resistance. An additional value of conductivity is calculated involving the hydrogel measurements; $\sigma = \frac{d}{R \cdot H \cdot W}$.[14] Where d is the distance between electrodes, R is the resistance obtained from the voltmeter, H is the height of the hydrogel sample and W is the width of the hydrogel sample. The resistance measurements were collected immediately after crosslinking and measured again after samples were soaked in PBS for five days.

2.2.2 Resolution of Hydrogels

Conductive and electroactive polymers will eventually be printed into complex scaffolds. Therefore, it is necessary to observe the printability of each solution. In particular, the resolution of these solutions was examined. Resolution tests were conducted on the electroactive polymer and different conductive polymers at varying increasing polymer concentrations using the Elegoo Mars 3 printer. 40 ml solutions were made and were mixed using a digital sonicator for 30 minutes. To conduct the resolution study, rectangles with dimensions 4.5mmx0.8mm x0.1mm are drawn on AutoCAD and sliced using the slicing software CHITUBOX. After printing the rectangular hydrogels, the sample's length, height, and width are measured. Three sets of measurements were taken, one on the printer plate, another once removed from the printer plate, and another after the samples were soaked in PBS for three days. The results were graphed on a bar graph. And measurements were compared to that from the AutoCAD drawing.

2.2.3 Biocompatibility of Hydrogels

The different conductive polymers hydrogels samples (n=6) were prepared and cut into 6mm circles. These circles were placed in 24 well culture plates and each side was exposed to UV light at a wavelength of 365 nm for 30 minutes each. After UV light exposure the samples were washed with 70% ethanol for one hour. Samples were further washed in sterile PBS for one hour. PBS was removed and samples were soaked in fetal bovine serum (FBS) for one hour. Afterward, the samples were incubated overnight in Dulbecco's Modified Eagle Medium (DMEM) with 10% fetal bovine serum, and 1% penicillin/streptomycin (P/S) at 37° C. The wells were seeded with 60,000 C2C12 mouse myoblasts cells per well (30,000 cells/cm^2) on day 0. PrestoBlue cell viability assay was used to quantify cellular metabolic activity and proliferation on 1,3, and 5 days after seeding to evaluate the sample's biocompatibility. Cells were incubated

for an hour with DMEM medium and 10% PrestoBlue at these time intervals. Absorbance was later measured using a Tecan Infinite M200 PRO plate reader at 570 nm.

2.2.4 Actuation of Hydrogel Sandwiches

Hydrogel samples were crosslinked in a PDMA mold measured 20mmx4mmx2mm, and conductive, electroactive hydrogel sandwiches were created. The first layer is the conductive layer, where CNT/DMF, gold particle solution, and $FeCl_3$ solution were mixed with a flexible resin, and crosslinked for 2 minutes. The conductive portions are made of a 1:1 conductive material solution: flexible resin mixture, 1 ml of conductive material solution, and 2 ml of flexible resin. To aid in eventual 3D printing commercially available, flexible 3D printing resin was added to the polymers. The SuperFlex flexible resin from 3D Materials has a balanced softness with strength. After the first conductive layer is crosslinked, the electroactive portion is added and crosslinked for 2 minutes. The electroactive portion is made of a 2:1 PEGDA/AA: Flexible Resin mixture, 2 ml of PEGDA:AA and 1 ml of flexible resin. After the electroactive portion is crosslinked, the final layer, the second conductive portion is added on top and crosslinked for 2 minutes. Each conductive material, (CNT, gold nanoparticle, and $FeCl_3$) has a conductive, electroactive, conductive hydrogel sandwich. The sandwich is cut into thirds and placed in the device created to measure the response to an electric field (Figure 1). The design is a petri dish filled with PBS, with two platinum electrodes 4 cm apart. The platinum electrodes are 99.5% pure and 0.20 mm in diameter, they are attached to both ends of the conductive layers. The samples are held using two small pegs in the middle of the petri dish and electrodes to hold them up. A DC voltage of 20 V, equivalent to 6.67 V/cm, was applied for 5 minutes at a time using an Agilent Dual Output DC Power Supply (E3646A Agilent Technologies, Santa Clara, CA, USA).[3] Three samples of each hydrogel sandwich, CNT, gold nanoparticles, and $FeCl_3$

hydrogels were measured, along with a control, which is a regular PEGDA/AA with resin mixture crosslinked. All actuation tests were recorded in video mode with a phone camera, and the videos were replayed and analyzed to determine the angular movement.[3]

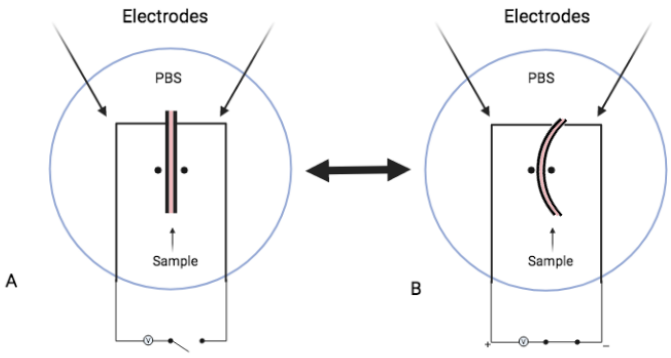

Figure 1: A)Petri dish set up for Actuation testing before 20V voltage is applied. The conductive electroactive portions are straight in the middle of the pegs and submerged in PBS. The platinum electrodes are attached to both sides of the conductive portion of the sandwich. B)Petri dish set up when 20V voltage is applied, the hydrogel bends toward the negative electrode

2.3 3D Printing

2.3.1 3D Printer

The hydrogel samples and scaffold design are printed using the Elegoo Mars 3 Ultra 4K Mono LCD Printer. It is the company's first ultra-4k high-precision, compacted-size desktop LCD resin 3D printer. It makes use of a new release film 2.0 for printing, an updated COB UV light source structure, and a 6.6-inch ultra-4K high-resolution monochrome LCD. The UV light operates at a wavelength of 405 nm and has a resolution of 4098 pixels*2560 pixels.[23]

2.3.1 Design/Print of the Scaffold

The scaffold is designed to resemble a sarcomere. The entire design will be 3D printed with a conductive material mixed with the flexible polymer. The scaffold was designed in AutoCAD

(Figure 2). The legs in the middle(A) represent myosin, and the space in the middle(B) represents the myosin heads which were filled with the electroactive hydrogel mixture and crosslinked. The line down the middle(C) represents the M line and (E) the lines at the end of myosin represent the actin, and the outer portions provide support for the scaffold (D, F). The scaffold is printed at 3mm and is sliced using the slicing software Chitubox. There are a total of 24 layers, and each layer has an exposure time of 120 seconds for a 48-minute print jobThe CNT/DMF is mixed with the flexible resin at a 2:1 ratio. 30 ml of CNT/DMF and 15 ml of the flexible resin mixture is sonicated for an hour. This mixture is then put into a vacuum overnight at 40 degrees Celsius and 15 mmHg for 5 hours to dissolve the DMF. This solution is then placed in the printer to print the scaffold.

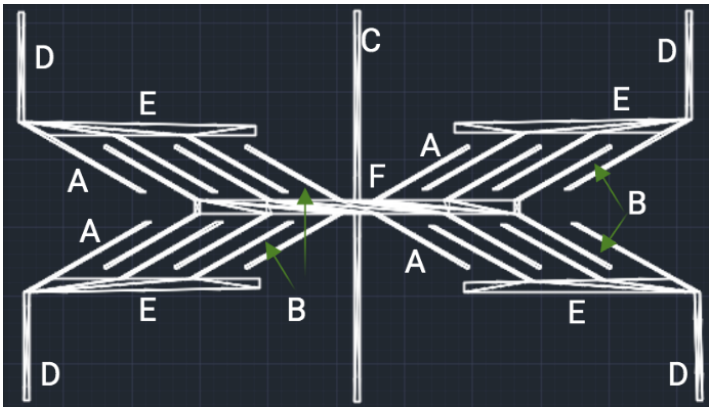

Figure 2: This scaffold is designed in Autocad to resemble a sarcomere. A, the legs of the scaffold represent the myosin filaments. B, the spaces in between the legs represent the myosin heads are filled with the electroactive portion. C is the M line, and E is the actin filaments, and the outer portions allow for support of the scaffold. (D, F)

2.4 Results

2.4.1 Conductivity

2.4.1.1 CNT Hydrogels

The resistance and conductivity of CNT, gold particle hydrogels and $FeCl_3$ hydrogels were collected at different concentrations. The concentrations were 1%,5%,10%,15%,30%, and 50%. Their conductivity was also compared to that of regular PEGDA/AA hydrogens with no conductive material. These values were collected immediately after crosslinking, and after the hydrogels were soaked in PBS for 5 days. In the CNT samples that were measured immediately after crosslinking the hydrogels measured with the addition of 20 V are much less resistant and much more conductive than those without a 20 V charge applied to them. As depicted in figure 3A results show no significant difference in conductivity from 1%-15%, however, there is a huge increase in conductivity from 15% to 30%. After these samples were soaked in PBS for 5 days, the results are depicted in Figure 3B.

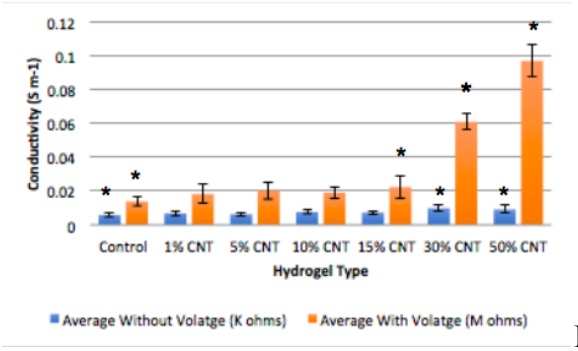

A.

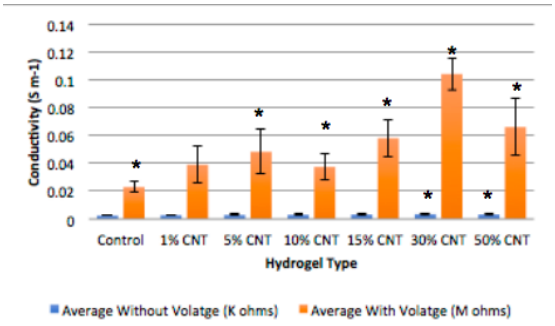

B.

Figure 3: PEGDA hydrogels with 1%-50% CNT concentration. A) Conductivity (S m-1) of carbon nanotube hydrogels immediately after crosslinking. There is no significant difference between control to 30%. There is even a slight decrease in conductivity at 15%. Large increase in conductivity at 30% and 50%. 30% is more than twice as much conductive as 15%, and there is nearly an increase of twice as much from 30% to 50%. B) Conductivity of carbon nanotube hydrogels after soaking in PBS for 5 days. There is a slight increase from control to 1% concentration and a slight decrease for 15%. Again there is a big increase in 30% concentration and then a decrease in conductivity of 50% concentration. The largest conductivity value is

observed at 30% concentration of CNT. (* indicates a statistically significant difference with $p < 0.05$).

2.4.1.2 Gold Hydrogels

The gold particle hydrogel results were as expected. As the concentrations of the gold particles in the PEGDA solutions increased, so did the conductivity. Figure 4A depicts a constant upward trend in conductivity as the concentrations increase, and also depicts the conductivity of the hydrogels soaked in PBS for 5 days (Figure 4B).

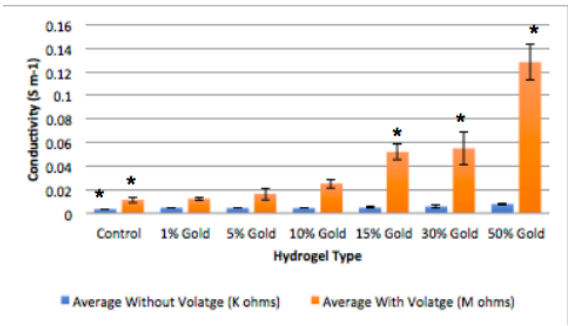

A.

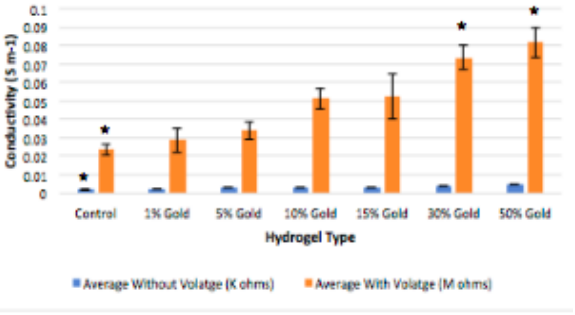

B.

Figure 4: PEGDA hydrogels with 1%-50% gold concentration. A) Conductivity (S m-1) of gold hydrogels immediately after crosslinking. The resistance values collected shared an inversely proportional relationship to the concentrations and conductivity values shared a directly proportional relationship. As the concentration of gold particles increased so did the conductivity. The biggest increase in conductivity was seen in the larger concentrations of the gold particles, particularly, 30% and 50%. B) Conductivity of gold hydrogels after soaking in PBS for 5 days. There is a constant increase in conductivity as the concentration increases. With 50% concentration recording the highest conductivity. (* indicates a statistically significant difference with $p < 0.05$).

2.4.1.3 $FeCl_3$ Hydrogels

The $FeCl_3$ hydrogels did not show much of a difference in conductivity as the $FeCl_3$ concentrations increased in the PEGDA solution as depicted in Figure 5A. After the hydrogels were soaked in PBS for five days, there are varying conductivity values as the $FeCl_3$ concentrations increase shown in Figure 5B.

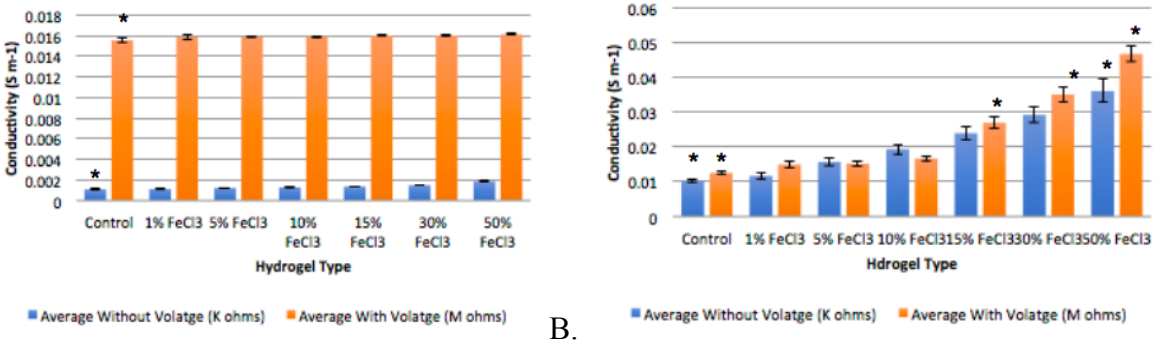

Figure 5: PEGDA hydrogels with 1%-50% $FeCl_3$ concentration. A) Conductivity (S m-1) of $FeCl_3$ hydrogels immediately after crosslinking. Immediately after crosslinking, there is no significant difference between $FeCl_3$ control-50% concentration. B) Conductivity of $FeCl_3$ hydrogels after soaking in PBS for 5 days. After soaking there is a directly proportional relationship between the $FeCl_3$ concentration to the conductivity of the hydrogel. As the concentrations increased so did the conductivity of the hydrogels, this is to be expected, and what was seen in the gold particle and CNT hydrogels. Again 50% concentration recorded the highest conductivity. (* indicates a statistically significant difference with $p < 0.05$).

2.4.2 Resolution

2.4.2.1 CNT Hydrogels

The length, width, and height of hydrogel samples with different conductive materials (CNT, gold particle, and $FeCl_3$) were measured to see the effects of 3D printing on the resolution of a design, as polymer concentrations increased. 4.5x0.8x0.1 rectangles were drawn on AutoCAD and printed using a 3D printer. The CNT samples did not show a significant difference in

dimensions as the polymer concentration increased (Figure 6A). After the hydrogels were removed from the printing plate the dimensions increased (Figure 6B). After soaking for 3 days in PBS, the hydrogels swelled, significantly changing the dimensions (Figure 6C)

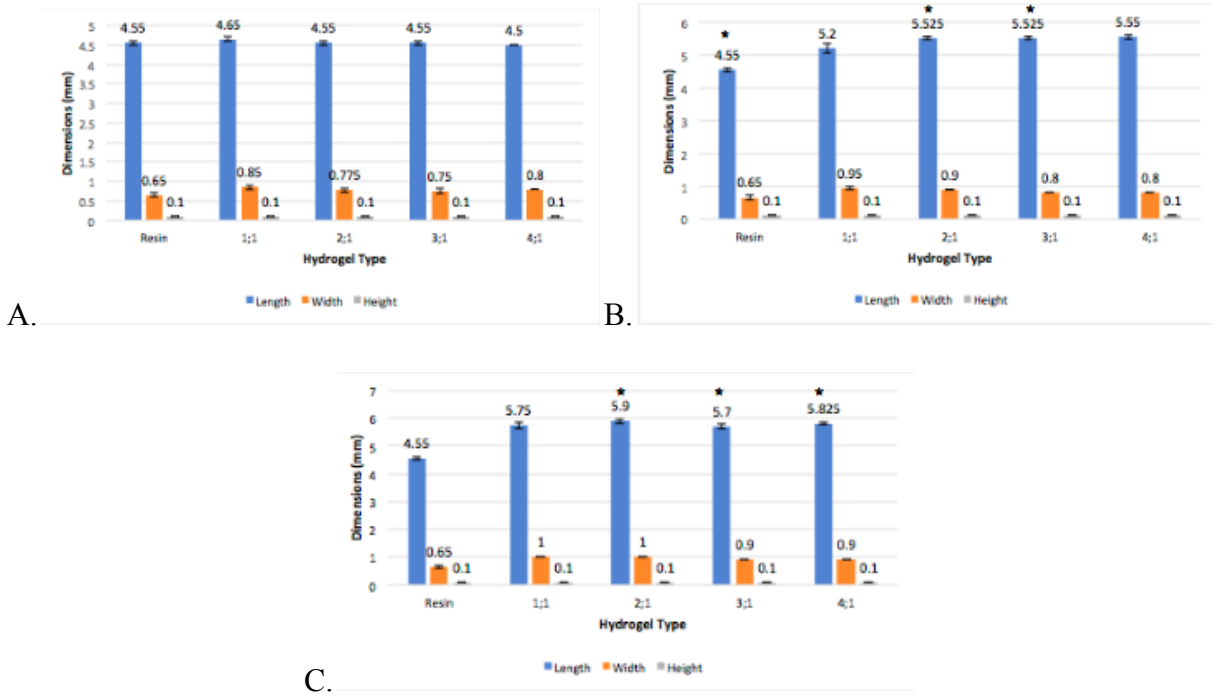

Figure 6: PEGDA hydrogels dimensions with carbon nanotubes. A) Hydrogel dimensions (mm) on the printer plate. There is no significant difference in the dimensions as the polymer concentration increases. However, the highest dimensions were recorded for the 1:1 ratio, and the most accurate being the 3:1 ratio. B) Hydrogel dimensions (mm) off the printer plate. After removing from the printer plate all dimensions increased. The largest change in dimensions is recorded with the 4:1 ratio hydrogels. C) Hydrogel dimensions (mm) after soaking in PBS for 3 days. The most significant change in dimensions is seen in the 2:1 ratio of hydrogels. (* indicates a statistically significant difference with $p < 0.05$).

2.4.2.2 Gold Hydrogels

Similarly to the CNT hydrogels, the gold particle hydrogels did not show a significant difference in dimensions as the polymer concentrations increased (Figure 7A). However, after being removed from the printer plate there was an increase in dimensions (Figure 7B). After soaking in PBS there was an even larger increase in dimension to all of the hydrogels, regardless of polymer concentration. (Figure 7C)

A.

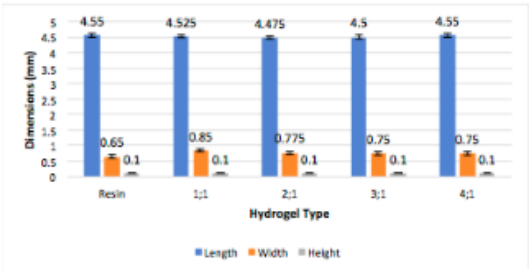

B.

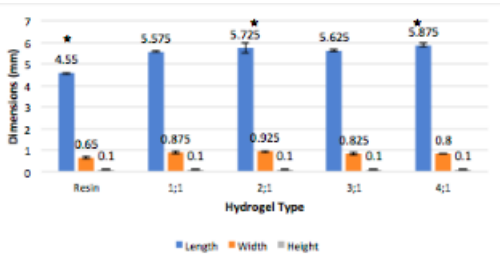

C.

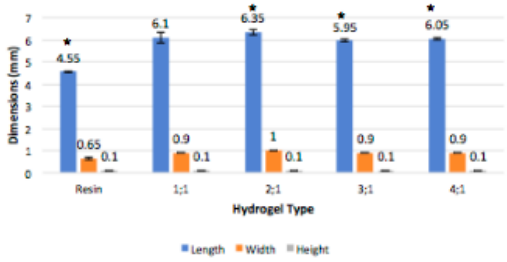

Figure 7: PEGDA hydrogels dimensions with gold nanoparticles. A) Hydrogel dimensions (mm) on the printer plate. There is no significant difference in the dimensions as the polymer concentration increases. However, the highest dimensions were recorded for the 4:1 ratio, and the most accurate being the 3:1 ratio. B) Hydrogel dimensions (mm) off the printer plate. After removing from the printer plate all dimensions increased. The largest change in dimensions is recorded with the 4:1 ratio hydrogels. C) Hydrogel dimensions (mm) after soaking in PBS for 3 days. The most significant change in dimensions is seen in the 2:1 ratio of hydrogels. (* indicates a statistically significant difference with $p < 0.05$).

2.4.2.3 PEGDA:AA Hydrogels

With the regular PEGDA hydrogels again there was no significant difference in the dimensions of the hydrogels on the printer plate as the polymer concentrations increased(Figure 8A). As the hydrogels were removed from the printer plate there were varying dimensional changes all of them higher than that of the printer plate. (Figure 8B). And after soaking for three days in PBS, the hydrogels dimensions increased due to swelling. (Figure 8C)

A..

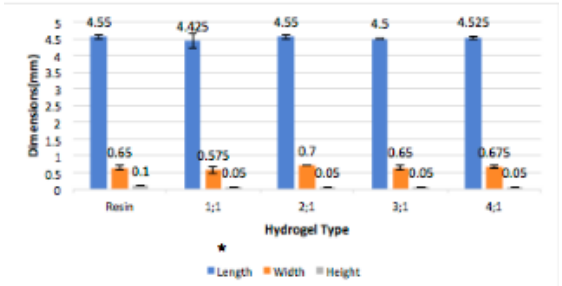

B.

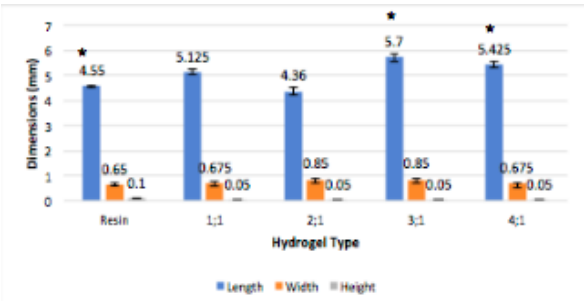

C.

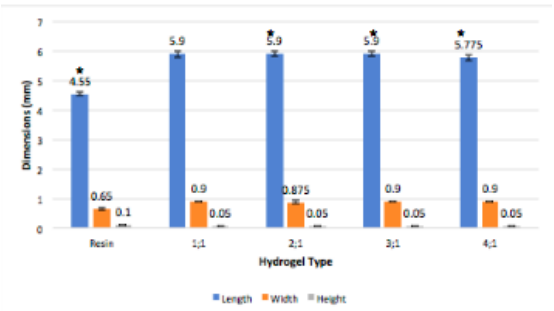

Figure 8: PEGDA hydrogels dimensions. A) Hydrogel dimensions (mm) on the printer plate. There is no significant difference in the dimensions as the polymer concentration increases. However, the highest dimensions were recorded for the 2:1 ratio, and the most accurate being the 3:1 ratio. B) Hydrogel dimensions (mm) off the printer plate. After removing from the printer plate all dimensions increased. The largest change in dimensions is recorded with the 3:1 ratio hydrogels. C) Hydrogel dimensions (mm) after soaking in PBS for 3 days. The most significant change in dimensions is seen in the 2:1 ratio of hydrogels. (* indicates a statistically significant difference with $p < 0.05$).

2.4.3 Biocompatibility

2.4.3.1 CNT Hydrogels

Presto blue cell viability was conducted on CNT hydrogels on 1,3, and 5 days of cell proliferation. Each group showed an increase in RFU as the number of days increased. The AA hydrogels had lower RFU numbers than the other hydrogels. (Figure 9)

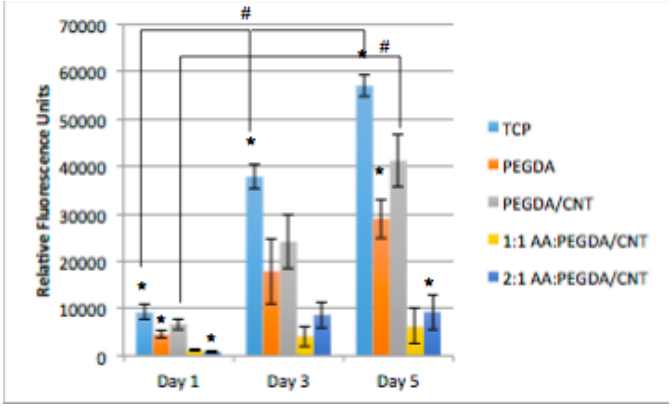

Figure 9: Metabolic Activity of Hydrogels, with and without carbon nanotubes. TCP, PEGDA, PEGDA/CNT, 1:1 AA: PEGDA/CNT, and 2:1 AA: PEGDA/CNT cell activity on hydrogels all increased as the days increased. Hydrogels with AA displayed the lowest RFU numbers and PEGDA/CNT displayed the highest RFU numbers, in comparison to PEGDA, and the PEGDA with AA. Between the two AA groups, 1:1 displayed the higher RFU numbers. (* indicates a statistically significant difference with $p < 0.05$). # indicates statistically significant from day 1 to day 5 in TCP and PEGDA/CNT

2.4.3.2 Gold Hydrogels

Presto Blue Cell viability was also conducted on the gold particle hydrogels on 1,3, and 5 days of cell proliferation. Each group showed an increase in RFU from day 1 to day 5 however differing groups had higher RFU numbers. The PEGDA and PEGDA/Gold groups had higher numbers than the hydrogels with 1:1 and 2:1 AA ratios. 2:1 shows lower numbers than 1:1. And the PEGDA/Gold shows higher RFU numbers than regular PEGDA. (Figure 10)

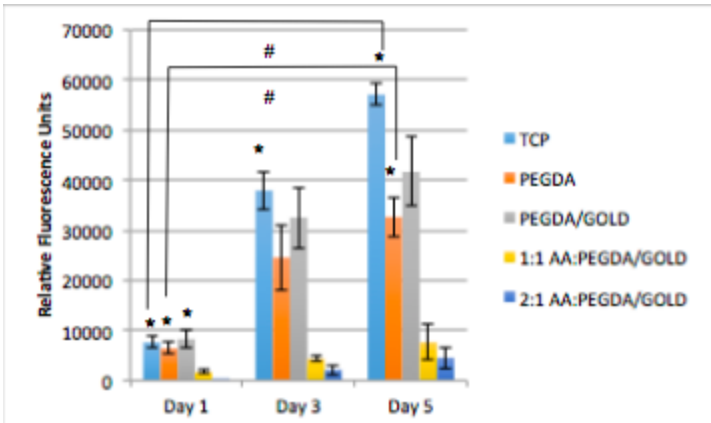

Figure 10: Metabolic Activity of Hydrogels, with and without gold particles. TCP, PEGDA, PEGDA/GOLD, 1:1 AA: PEGDA/Gold, and 2:1 AA: PEGDA/Gold cell activity on hydrogels all increased as the days increased. Hydrogels with AA displayed the lowest RFU numbers and PEGDA/Gold displayed the highest RFU numbers, in comparison to PEGDA, and the PEGDA with AA. Between the two AA groups, 1:1 displayed the higher RFU numbers. (* indicates a statistically significant difference with $p < 0.05$). # indicates statistically significant from day 1 to day 5 in TCP and PEGDA

2.4.3.3 $FeCl_3$ Hydrogels

Presto blue cell viability was on $FeCl_3$ hydrogels. Again here each group showed an increase in RFU as the number of days increased. 1:1 PEGDA/$FeCl_3$ showed the biggest increase in RFU as the days increased. And the hydrogels with the $FeCl_3$ were higher than that of the regular hydrogels. (Figure 11)

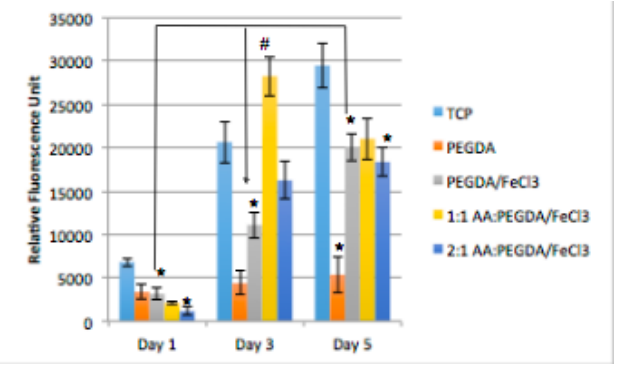

Figure 11: Metabolic Activity of Hydrogels, with and without carbon nanotubes. TCP, PEGDA, PEGDA/$FeCl_3$, 1:1 AA: PEGDA, and 2:1 AA: PEGDA/$FeCl_3$ cell activity on hydrogels all increased as the days increased, except for 1:1 AA: PEGDA/$FeCl_3$ that showed a decrease in Day 5. Hydrogels with AA displayed higher RFU numbers in comparison to PEGDA and PEGDA/$FeCl_3$. Between the two AA groups, 2:1 displayed the higher RFU numbers.(* indicates a statistically significant difference with $p < 0.05$). # indicates statistically significant from day 1 to day 5 in PEGDA/$FeCl_3$

2.4.4 Actuation

Actuation studies were done on regular PEGDA: AA hydrogels with resin, and CNT, gold nanoparticle, $FeCl_3$ conductive electroactive sandwiches. The CNT sandwich experienced the most movement and curvature, as it had the highest angular movement. The PEGDA: AA hydrogels were a close second as seen in Figure (12)

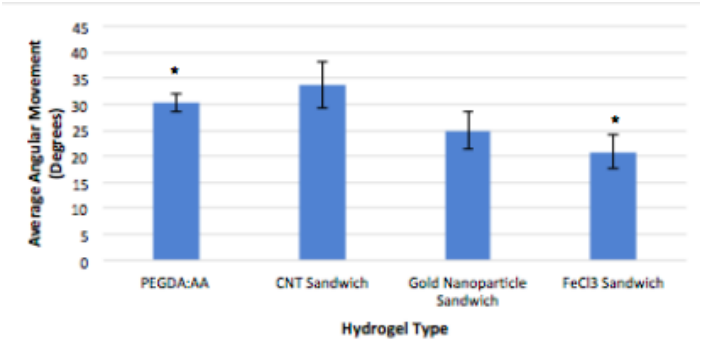

Figure 12: Actuation Testing of Hydrogels. CNT hydrogels resulted in the highest average number of angular movement at 33.7º. The PEGDA: AA hydrogels are a close second with 30.23º. The gold nanoparticle hydrogels recorded an average of 24.96º, and the $FeCl_3$ hydrogels came in last with an average of 20.83º. (* indicates a statistically significant difference with $p < 0.05$).

2.5 Discussion

2.5.1 Conductivity

The largest increase in conductivity was seen in the 15%-50% concentrations of the CNT, gold particle, and $FeCl_3$ hydrogels which is to be expected (Figure 13). As the concentrations of the conductive material increased so did the conductivity. Comparing the higher concentrations of the conductive material to the PEGDA solution we see the largest conductivity recorded at 50% $FeCl_3$, 50% gold particle, and 30% CNT. The highest conductivity overall was recorded for 30% CNT. Though the highest conductivities were recorded at higher concentration values, it is important to find a balance between high conductivity and lower concentration values, as it may be more beneficial for biocompatibility reasons. In this case, a 30% CNT hydrogel is the most optimal option.

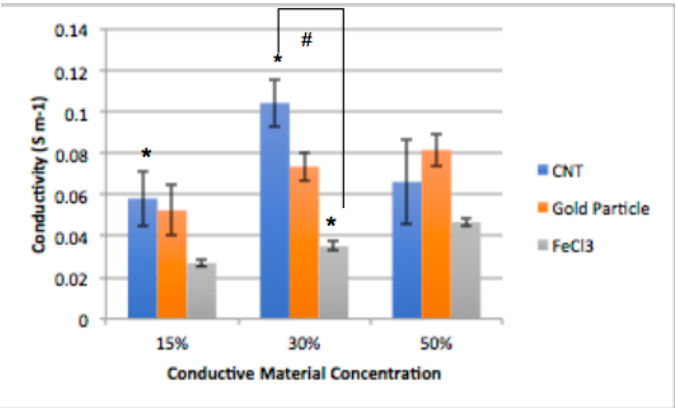

Figure 13: Conductivity with voltage applied, of CNT, gold particles, and FeCl3 hydrogels. Highest conductivity recorded at 30% CNT concentration. # indicates statistically significant from the PEGDA/conductive, 1:1 AA;PEGDA./conductive, 2:1 AA:PEGDA/conductive. (* indicates a statistically significant difference with $p < 0.05$). # indicates statistically significant from CNT to $FeCl_3$

2.5.2 Resolution

After hydrogels were removed from the printer plate, the dimensions increased which is to be expected as they are no longer bound to a metal surface. The regular hydrogels showed an average percent increase of 14.5%. The CNT hydrogels showed a percent increase of 20.83% and the gold hydrogels showed a percent increase from 26.7%. PEGDA:AA hydrogels had the lowest average, and CNT hydrogels the second lowest. This is important to note for the future when designing artificial muscle scaffolds. 3D printing can affect the dimension of your design. After hydrogels were soaked in the PBS, there was a great amount of swelling in all hydrogels (with and without conductive materials). However, the 2:1 hydrogels showed the largest increase and swelling of hydrogels, as compared to the 3:1 and 4:1. This can be due to the lower cross-link density in the 2:1 PEGDA: AA group. Regular hydrogels showed an average percent of 28.7%, CNT hydrogels 30.3% increase, and gold hydrogels 35.3% increase. PEGDA:AA hydrogels, and CNT hydrogels showing the least change in dimensions, making $FeCl_3$ and CNT hydrogels the optimal options.

2.5.3 Biocompatibility

In each of the groups, TCP, PEGDA, PEGDA/Conductive material, 1:1 PEGDA/Conductive material: AA, and 2:1 PEGDA/Conductive material: AA depicted an increase in RFU from day 1 to day 5. The PEGDA with each of the conductive materials showed higher RFU numbers and biocompatibility than just the regular hydrogels (Figure 14). PEGDA alone isn't the most viable environment for cells, cells have issues binding to its surface, so adding a conductive material may alter the environment and give them a surface more conducive for cellular binding proteins. This makes for a better environment for the cells and increases their viability. Adding AA to the hydrogels decreased biocompatibility compared to the PEGDA hydrogel, and conductive material, however, the 1:1 ratio showed higher cell viability than 2:1 hydrogels. This is to be

expected as acrylic acid is also not the best optimal environment for cells as it can alter the local pH, making it more acidic. The CNT, and gold hydrogels have the highest RFU in the PEGDA/Conductive material group making them the most compatible and the optimal options.

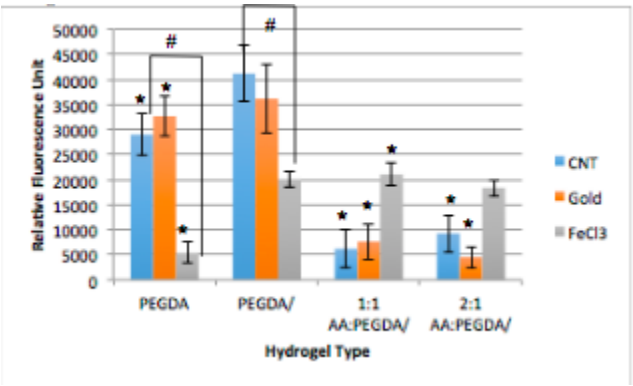

Figure 14: Metabolic Activity of Hydrogels. Day 5 RFU values, for PEGDA, PEGDA/conductive, 1:1 AA;PEGDA./conductive, 2:1 AA:PEGDA/conductive. PEGDA/Conductive materials are the most biocompatible group. Within this group we see that CNT, and gold have higher cell activity than $FeCl_3$. # indicates statistically significant from the PEGDA CNT to $FeCl_3$, and PEGDA/conductive from CNT to $FeCl_3$ (* indicates a statistically significant difference with $p < 0.05$).

2.5.3.4 Actuation

It was expected that the PEGDA: AA hydrogels would record the highest angular movement because it is just one layer of the electroactive hydrogels, the electrodes were attached directly to it, allowing for direct voltage stimulation and quicker and more angular movement. Though it recorded a higher angular movement, the CNT hydrogels recorded the highest. They had a high angular movement even though it is a 3-layer sandwich meaning it is thicker and does not receive direct voltage stimulation to the electroactive middle layer. The gold nanoparticle hydrogels and the $FeCl_3$ hydrogels had lower angular movements, this can be due to the thick

consistency of the hydrogels after crosslinking which can make it more difficult for the hydrogel to curve and move as well as the decreased conductivity compared to the CNT hydrogels.

CHAPTER 3 - Conclusions and Future Direction

Conclusions

In this study, CNT hydrogels, gold particle hydrogels, and $FeCl_3$ hydrogels were produced and tested for their conductivity, resolution, and biocompatibility. The largest conductivity values were seen in the 15%-50% conductive material concentration. Overall CNT and Gold particles create higher conductivity compared to $FeCl_3$. CNT hydrogels are the most conducive with 15% and %30, depicting CNT to be slightly more conductive than gold particles. Resolution studies showed that PEGDA:AA hydrogels AND CNT hydrogels had the lowest percent change in dimension of the hydrogels. This is important when 3D printing CNT hydrogels may be optimal. It is important to note the changes in dimension for CNT if planning to 3D print with CNT hydrogels. Biocompatibility findings were similar for all three conductive materials, adding the conductive material created a much more viable environment for the cells than just PEGDA hydrogels, however adding AA, which creates an electroactive polymer, the cells are less viable. And adding more AA allows for an even less viable environment. The most biocompatible environment is the CNT and PEGDA hydrogels. Overall CNT hydrogels came out to be the most optimal conductive material composite to use for the electroactive and conductive muscle scaffold.

Future Work

The findings from this study can be used to 3D print an artificial muscle scaffold resembling the structure of a sarcomere, with the actin and myosin filaments that move. The use of a combination of electroactive polymers (EAPs) and conductive materials can serve as great

muscle scaffolds because of their ability to mimic native muscle with its mechanical and contractile properties. The findings of the best conductive material added to Electroactive polymers, with the most accurate 3D printing scaffold, and the best biocompatible option can help create and 3D print this artificial muscle scaffold. From the results, carbon nanotubes are the most optimal option to use as the conductive material for the 3D. Using the Elegoo Mars 3 3D printer, the scaffold is printed, with the CNT: Resin solution. The electroactive material is then inserted into the legs and crosslinked. The platinum electrodes are inserted into outer support links, to introduce a voltage and induce movement and bending similar to the sliding filament model. In the future, it is beneficial to experiment with applying higher voltage and changing the design. A design with less conductive material and more electroactive may help with bending. Microscaling design can help with movement, and working with polymers without flexible resin can aid in biocompatibility. The work done has aided to create a scaffold that mimics the in vitro environment of muscle tissue development, which can lead to a scaffold that can be used as a graft to restore damaged muscle tissue.

Works Cited

1. AL;, McCuller C;Jessu R;Callahan. “Physiology, Skeletal Muscle.” *National Center for Biotechnology Information*, U.S. National Library of Medicine, https://pubmed.ncbi.nlm.nih.gov/30725824/.
2. Bar-Cohen, Y. (n.d.). *Chapter 01 Vincent - Electroactive polymers as artificial muscles* . Retrieved December 12, 2022, from https://www.witpress.com/Secure/elibrary/papers/9781853129414/9781853129414004FU1.pdf (13)
3. Browe,Daniel P. , Wood,Caroline, Sze,Matthew T., White,Kristopher A.,Scott,Tracy, Olabisi,Ronke M., Freeman,Joseph W. Characterization and optimization of actuating poly(ethylene glycol) diacrylate/acrylic acid hydrogels as artificial muscles,https://www.sciencedirect.com/science/article/pii/S0032386117304226 (18)
4. Burgoyne, T., Morris, E. P., & Luther, P. K. (2015, November 6). *Three-dimensional structure of vertebrate muscle Z-band: The small-square lattice Z-band in rat cardiac muscle*. Journal of molecular biology. Retrieved December 12, 2022, from https://www.ncbi.nlm.nih.gov/pmc/articles/PMC4641244/ (21)
5. Deyne, P. G. D., Orthopedics, D. of, LC, A., R, A., E, B., FW, B., A, B., K, B., VJ, C., JA, C., ER, C., JA, C., MS, C., GA, D., GM, D., JX, D. M., S, D., HF, E., M, F.-S., … Chun, L. G. (2000, December 1). *Formation of sarcomeres in developing myotubes: Role of mechanical stretch and contractile activation*. American Journal of Physiology-Cell Physiology. Retrieved December 12, 2022, from https://journals.physiology.org/doi/full/10.1152/ajpcell.2000.279.6.C1801 (7)
6. *Elegoo Mars 3 ultra 4K MONO LCD 3D printer*. ELEGOO Official. (n.d.). Retrieved December 12, 2022, from https://www.elegoo.com/products/elegoo-mars-3-lcd-3d-printer (23)
7. Foroughi, J., & Spinks, G. (2019, October 30). *Carbon nanotube and graphene fiber artificial muscles*. Nanoscale Advances. Retrieved December 12, 2022, from https://pubs.rsc.org/en/content/articlelanding/2019/na/c9na00038k (15)
8. Guo, B., & Ma, P. X. (2018, June 11). *Conducting polymers for Tissue Engineering*. Biomacromolecules. Retrieved December 12, 2022, from https://www.ncbi.nlm.nih.gov/pmc/articles/PMC6211800/ (12)
9. Khodabukus, A. (2021, February 26). *Tissue-engineered skeletal muscle models to study muscle function, plasticity, and disease*. Frontiers in physiology. Retrieved December 12, 2022, from https://www.ncbi.nlm.nih.gov/pmc/articles/PMC7952620/ (20)
10. Kim, G., & Kim, J. H. (2020, March). *Impact of skeletal muscle mass on metabolic health*. Endocrinology and metabolism (Seoul, Korea). Retrieved December 12, 2022, from https://www.ncbi.nlm.nih.gov/pmc/articles/PMC7090295/ (6)
11. Liu, J., Saul, D., Böker, K. O., Ernst, J., Lehman, W., & Schilling, A. F. (2018, April 16). *Current methods for skeletal muscle tissue repair and regeneration*. BioMed research international. Retrieved December 12, 2022, from https://www.ncbi.nlm.nih.gov/pmc/articles/PMC5926523/ (4)
12. Mihajlovic, M., Mihajlovic, M., Dankers, P. Y. W., Masereeuw, R., Sijbesma, R. P., *Macromol. Biosci.* 2018, 1800173. https://doi.org/10.1002/mabi.201800173 (14)

13. Naghdi, S., Rhee, K. Y., Hui, D., & Park, S. J. (2018, August 9). *A review of conductive metal nanomaterials as conductive, transparent, and flexible coatings, thin films, and conductive fillers: Different deposition methods and applications*. MDPI. Retrieved December 12, 2022, from https://www.mdpi.com/2079-6412/8/8/278 (17)
14. Owings M, Kozak LJ, National Center for Health S. Ambulatory and Inpatient Procedures in the United States, 1996. Hyattsville, Md.: U.S. Dept. of Health and Human Services, Centers for Disease Control and Prevention, National Center for Health Statistics; 1998. https://pubmed.ncbi.nlm.nih.gov/9540438/ (2)
15. Eckardt, André., Fokas,Konstantinos.,Microsurgical reconstruction in the head and neck region: an 18-year experience with 500 consecutive cases, Journal of Cranio-Maxillofacial Surgery.https://www.sciencedirect.com/science/article/pii/S1010518203000398 (8)
16. Ruonan Dong, Peter X. Ma, Baolin Guo, Conductive biomaterials for muscle tissue engineering, Biomaterials, https://www.sciencedirect.com/science/article/pii/S0142961219306830 (19)
17. Rizzi, R., Bearzi, C., Mauretti, A., Bernardini, S., Cannata, S., & Gargioli, C. (2012, October 16). *Tissue engineering for skeletal muscle regeneration*. Muscles, ligaments and tendons journal. Retrieved December 12, 2022, from https://www.ncbi.nlm.nih.gov/pmc/articles/PMC3666528/ (11)
18. Sellers 2004 (22)
19. Shin, M., Choi, J.-H., Lim, J., Cho, S., Ha, T., Jeong, J. H., & Choi, J.-W. (2022, May 25). *Electroactive nano-biohybrid actuator composed of gold nanoparticle-embedded muscle bundle on molybdenum disulfide nanosheet-modified electrode for motion enhancement of Biohybrid Robot - Nano Convergence*. SpringerOpen. Retrieved December 12, 2022, from https://nanoconvergencejournal.springeropen.com/articles/10.1186/s40580-022-00316-8 (16)
20. Sicari, B. M., Rubin, J. P., Dearth, C. L., Wolf, M. T., Ambrosio, F., Boninger, M., Turner, N. J., Weber, D. J., Simpson, T. W., Wyse, A., Brown, E. H. P., Dziki, J. L., Fisher, L. E., Brown, S., & Badylak, S. F. (2014, April 30). *An acellular biologic scaffold promotes skeletal muscle formation in mice and humans with volumetric muscle loss*. Science translational medicine. Retrieved December 12, 2022, from https://www.ncbi.nlm.nih.gov/pmc/articles/PMC5942588/ (10)
21. Tedesco, F. S., Dellavalle, A., Diaz-Manera, J., Messina, G., & Cossu, G. (2010, January). *Repairing skeletal muscle: Regenerative potential of skeletal muscle stem cells*. The Journal of clinical investigation. Retrieved December 12, 2022, from https://www.ncbi.nlm.nih.gov/pmc/articles/PMC2798695/ (3)
22. Wang, X. H., Du, J., Klein, J. D., Bailey, J. L., & Mitch, W. E. (2009, October). *Exercise ameliorates chronic kidney disease-induced defects in muscle protein metabolism and progenitor cell function*. Kidney international. Retrieved December 12, 2022, from https://www.ncbi.nlm.nih.gov/pmc/articles/PMC3835682/ (9)
23. Yiu, E. M., & Kornberg, A. J. (n.d.). *Duchenne muscular dystrophy - yiu - 2015 - wiley online library*. Retrieved December 12, 2022, from https://onlinelibrary.wiley.com/doi/10.1111/jpc.12868 (5)

24. Ziegler-Graham K, MacKenzie EJ, Ephraim PL, Travison TG, Brookmeyer R. Estimating the Prevalence of Limb Loss in the United States: 2005 to 2050. Archives of Physical Medicine and Rehabilitation2008;89(3):422-9. https://pubmed.ncbi.nlm.nih.gov/18295618/ (1)